Exploiting the relation between users' mental state and performance in a Brain Computer Interface setting

Cecilia Maeder [1]

On-Site Supervisor: Dr. Benjamin Blankertz [1,2]
Second Reader: Prof. Dr. Peter Desain [3]
Other authors: C. Sannelli [1], S. Haufe [1]

[1] Berlin Institute of Technology, Machine Learning Laboratory, Berlin, Germany
[2] Fraunhofer FIRST, Berlin, Germany
[3] Donders Institute for Brain, Cognition and Behaviour, Nijmegen, the Netherlands

Correspondance to: Cecilia Maeder, e-mail: ceciliamaeder@gmail.com

Abstract

High amplitudes in the 8-15 Hz frequency band over sensorimotor areas (sensorimotor rhythms, SMR) have been correlated with better sensorimotor processing and hypothesized to be due to higher inhibition to external inputs. In this study, we analyze data acquired during motor imagery of the right and left hands in an SMR based BCI setting and show that trials with higher SMR amplitude in the 1000 ms preceding the cue could be better classified than trials with lower amplitude. We also report that this increase in accuracy can be attributed to a higher level of SMR amplitude over the ipsilateral hemisphere. Finally, we conducted an online study in which the pre-stimulus SMR level controlled the timing of cue presentation. Preliminary results from this study are presented here and technical issues for future designs incorporating the monitoring of users ongoing SMR activity are discussed.

1 Introduction

1.1 Mental state and performance

Quantification of oscillatory brain activity in different frequency bands has been widely used in the investigation of mental states. More precisely, the influence of these rhythms preceding task begin on the outcome performance has been extensively studied and different effects have been reported. A first body of evidence links lower amplitudes in the α frequency band (8-14 Hz) over occipital areas to better perception in visual discrimination tasks (Ergenoglu et al., 2004; Hanslmayr, Klimesch, et al., 2005; Dijk, Schoffelen, Oostenveld, & Jensen, 2008). Similar effects are also reported for rhythmic activity in this frequency band over the perirolandic areas (labeled μ-rhythm or sensorimotor rhythms/SMR). However, in this case, several studies report a U-shaped relationship between amplitude in the μ-band and

somatosensory perception (Palva & Palva, 2007; Zhang & Ding, 2010). As high activity in this frequency band has been linked to idle of the cortical structures i.e. no active processing (Klimesch, Vogt, & Doppelmayr, 1999; Hummel, Andres, Altenmuller, Dichgans, & Gerloff, 2002), smaller amplitudes may reflect cortical activation and would mean that the sensory cortices involved in the task need to be in an appropriate excitation stage to process extrenal stimuli.

On the other side, α-band activity over frontal and posterior sites during resting state, have been demonstrated to correlate with performance in tasks requiring memory or higher cognitive processing (see (Klimesch, 1999) for a review). Going even further, some studies demonstrated that cognitive performance could be increased if the amplitude of the pre-stimulus α-band activity in parietal and frontal electrodes was enhanced artificially, e.g. by external stimulation (flickering of a target on a screen or repetitive Transcranial Magnetic Stimulation, rTMS) or operant conditioning (Hanslmayr, Sauseng, Doppelmayr, Schabus, & Klimesch, 2005; Klimesch, Sauseng, & Gerloff, 2003). This suggests that a high level of cortical activation will be helpful to analyze external inputs (e.g. visual, or somatosensory), but that this activation can be detrimental in the case of higher cognitive tasks, as it may interfere with (or even suppress) the high selectivity that is required for these processes.

In line with the previous findings, higher SMR amplitudes have been linked to better sensorimotor processing (Del Percio et al., 2007), but also to less accurate inhibition of motor responses (Mazaheri, Nieuwenhuis, Dijk, & Jensen, 2009). This supports the assumption that higher amplitudes in the α-band represent cortical deactivation, leading to inhibition of inputs from other areas. Hence accurate sensorimotor processsing seems to benefit from this inhibition. We expect this to result from the straight-forward porcessing of the motor programs, while abrupt changes of these motor programs (for inhibiting motor responses for example) is impaired due to the inhibition of external inputs inducing those changes.

1.2 Link to Brain Computer Interface Technology

Amplitude modulations over the sensorimotor cortices in the α-band and sometimes 13-28 Hz β-band (corresponding to the SMR) induced by motor imagery are commonly used in EEG based Brain Computer Interface (BCI) technology. Typically, due to topographical arrangement in the motor and somatosensory cortices, a decrease in amplitude, labeled event-related desynchronization (ERD), is observed over the cortical area corresponding to the used limb in the contralateral hemisphere; while an increase in amplitude, labeled event-related synchronization (ERS), is observed over the corresponding area in the ipsilateral hemisphere as well as the non-corresponding areas in both hemispheres (Pfurtscheller & Silva, 1999; Neuper & Pfurtscheller, 2001). This is described as the "focal ERD/surround ERS phenomenon (Suffczynski, Kalitzin, Pfurtscheller, & Silva, 2001; Pfurtscheller & Silva, 1999). Using modern machine learning techniques, the imagery of a subset of limbs (including the right and left hands, both feet and the tongue) can be discriminated (Pfurtscheller, Neuper, Flotzinger, & Pregenzer, 1997) and have been used in laboratory environments to control different types of assistive technologies like spellers (Blankertz et al., 2006, 2007), navigation systems (Millàn, Renkens, Mouriño, & Gerstner, 2004; Pfurtscheller et al., 2006) and neuroprosthetics (Pfurtscheller, Guger, Müller, Krausz, & Neuper, 2000; Enzinger et al., 2008). Figure 1 describes the amplitude modulations in the SMR band observed after motor imagery of the right and the left hand.

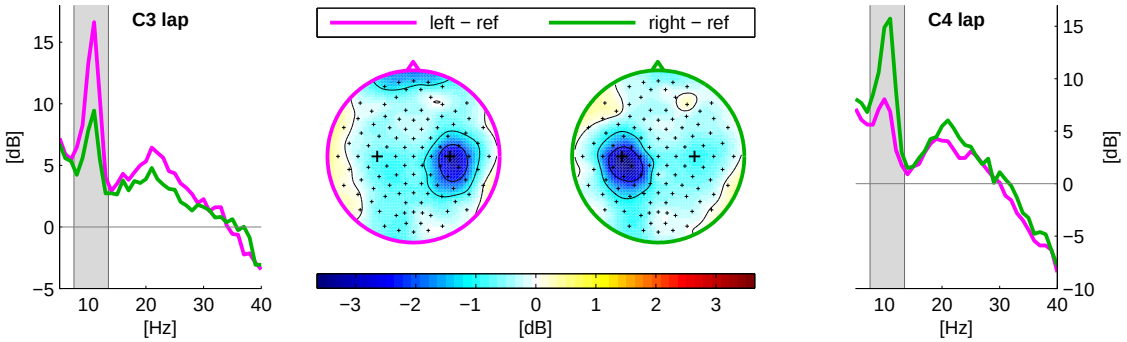

Figure 1: Event related desynchronization (ERD) during motor imagery of the left (purple) and the right hand (green). The left and right panels show the attenuation of the spectral power in the SMR band(s) (8-14 and 13-28 Hz) following motor imagery in two Lapacian filtered channels over the left (C4 lap) and the right (C3 lap) hemisphere. The central panel shows scalp topographies of these spectral attenuations. After imagery of the left hand, an ERD is observed over the right hemisphere and the opposite is observed for the right hand. Note that in this case no ipsilateral ERS is visible, which might be due to the baseline used.

Still, performance can vary extensively between sessions and even trials for the same user. We hypothesize that part of this variability could be attributed to ongoing fluctuations of the SMR, leading to more or less inhibition of the task-unrelated motor areas. The idea is that a higher SMR amplitude over the whole motor cortex preceding motor imagery would lead to spectral modulations over the task related limb area only, inducing a clear focal ERD/surround ERS pattern (Suffczynski et al., 2001; Pfurtscheller & Silva, 1999; Neuper & Pfurtscheller, 2001), which are easier to categorize. Supporting this assumption, Blankertz et al. developed a predictor showing a positive correlation of the SMR amplitude in a rest condition with BCI feedback performance (Blankertz et al., 2010). Following this, our study aims at demonstrating that there is a link between the actual state the user is in (mental state, (pre-) disposition, concentration, etc..) and his/her performance in a BCI setting and that this link could be exploited to boost performance.

2 Methods

2.1 EEG recording and preprocessing

Brain activity was recorded from the scalp using 119 Ag/AgCl electrodes, and sampled at 100 Hz.

Subject-specific frequency band and time interval were selected on calibration data using an automatic procedure comparing signed r-squared scores for each electrode over the motor cortex, for each frequency and time point. This method is described in (Blankertz, Tomioka, Lemm, Kawanabe, & Müller, 2008). The continuous EEG data was band-pass filtered and segmented into epochs according to the chosen frequency band and time interval. A variance based automatic artifact rejection was used to reject trials and channels with evident amplitude abnormalities.

2.2 Quantifying the SMR level

In order to investigate the effect of the ongoing SMR activity on the spectral modulations induced by motor imagery in a BCI setting, we use two different methods to quantify the SMR level:

- **Log SMR Band Power (*SMR Pow*)**
  The *SMR Pow* value is computed by averaging the log power in the subject-specific SMR frequency band over the two electrodes (one positioned over each motor area) exhibiting the highest discriminative score between the two classes. This is the standard method by which the SMR level is mostly quantified. We use this in the offline analysis.

- **Extracted SMR Ratio (*SMR Ratio*)**
  In order to achive a robust quantification of the ongoing SMR in an online BCI setting, we developed an *SMR extractor* to extract the *SMR Ratio* value directly from the recorded EEG signal. This consists of several several steps. Using a separate rest measurment, we first determine several subject-specific parameters (electrodes, frequency band and SMR range). The higher SMR peak in the μ (6-18 Hz) or in the β (15-35 Hz) defines the *start band*. It is then iteratively increased and decreased until the measure quantifying the peak area relative to its width does not increase anymore and yields the *SMR peak-band*. After this calibration, the mean power over the 2 Hz preceding and 3 Hz immediately following the *SMR peak-band* is subtracted from the power in this band. These power ratios are then averaged over the two chosen electrodes displaying the highest relative SMR-peak area values and normalized to the subject-specific SMR range. The *SMR Ratio* consists of this value averaged over a long (7500 ms) or a short (750 ms) time scale.

  Figure 2 illustrates the electrode and frequency band selection process.

2.3 Common Spatial Pattern Analysis and its use for classification

Common spatial pattern (see (Koles, 1991; Fukunaga, 1990; Blankertz et al., 2008)) is a discriminiative algorithm used to analyze multichannel EEG data recorded from two conditions (classes). It has shown to be a highly valuable tool for single trial classification of SMR modulations induced by motor imagery.

CSP analysis operates in a data driven supervised manner, allowing the identification of spatial filters, which maximize the variance of the signals in one condition, while minimizing it for the other condition. Since the variance of a band pass filtered signal equal to band power, CSP filters are well suited to detect spatiotemporal amplitude modulations of the SMR induced by motor imagery. The CSP algorithm decomposes band-pass filtered data in the sensor space, yielding as many spatial filters as sensors. The filters which have the best discriminative values are then selected based on their generalized eigenvalue. This is relative to the sum of the variance in both conditions. An eigenvalue near 1 corresponds to a high variance in the data for class 1, while an eigenvalue close to 0 means a small variance for class 1. Figure 3 illustrates the computation of the CSP filters based on data from two classes of motor imagery (left and right hand). Commonly, the two or three CSP filters with the highest discriminative value are determined for each class.

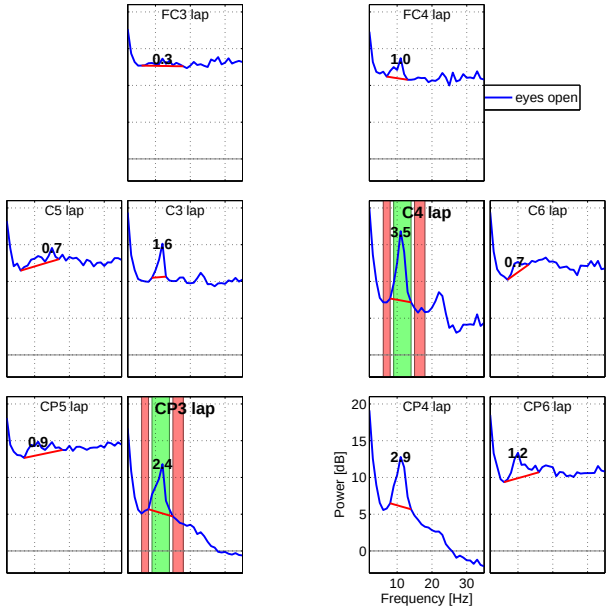

Figure 2: Illustration of the electrode and frequency bands selection for monitoring the SMR in one participant. The spectra are shown for the pre-defined electrodes the algorithm could select from.The algorithm choses one electrode per hemisphere with the highest SMR peak and then selects the frequency band around the peak (*SMR peak*-band in green), the neighboring bands (the *low*-band ([-2 0] Hz) and the *higher*-band ([0 3] Hz), in red). Note that this selection is performed on a performed on a separate rest measurment where the participant rests with open eyes and watches an animation gradually changing color and shape on a screen.

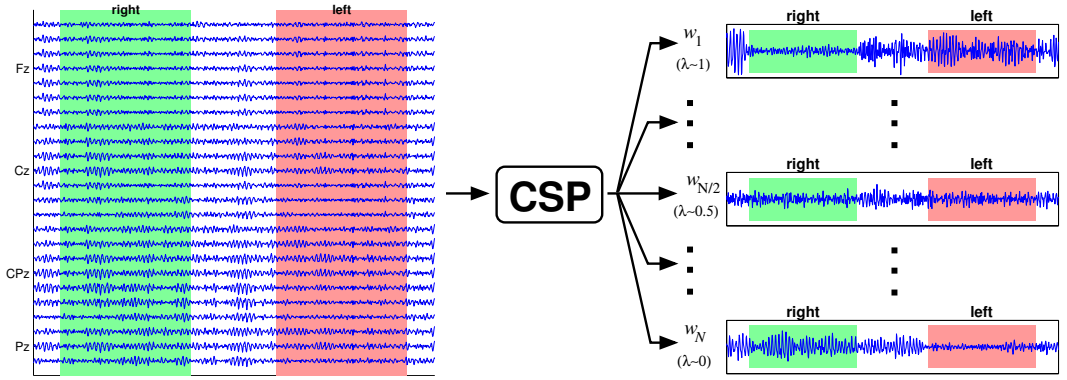

Figure 3: In this example, CSP analysis operates on band-filtered multi-channel EEG data recorded from two conditions of motor imagery (left and right hand colored in green, sepectively red). The analysis yields a sequence of spatial filters among which some have a high discriminative value between the two classes and others (most of them) do not. The filters with the highest discirminative value correspond to the ones with the extreme eigenvalues λ (top and bottom filters), while the filters with λ around 0.5 (central filter) have very little dicriminative power. Commonly, the two or three CSP filters with the highest discriminative value are selected for each class. Figure modified from (Blankertz et al., 2009).

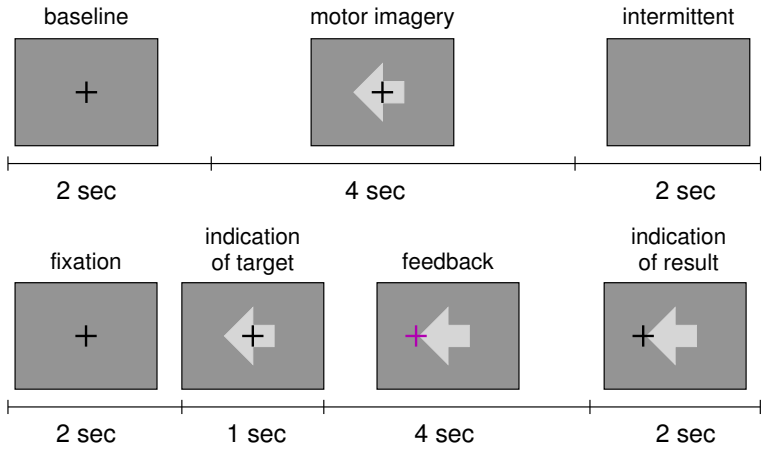

Figure 4: Timing and description of a calibration and a feedback trial in a standard motor imagery paradigm. Top panel: a *calibration* trial. In this type of trial, a baseline is shown for 2 seconds, followed by the presentation of a cue in form of an arrow indicating the hand the motor imagery should be performed with. The users performs motor imagery without feedback until the cue disappears. Bottom: a *feedback* trial. In this case, the cue is shown for 5 seconds and after one second, feedback is provided in the form of a purple cross moving according to the classifier output. After 4 seconds, the cross turns black and stops moving, which signifies the end of the trial. The end position of the feedback is shown for 2 seconds, followed by the start of the next trial.

Using CSP for classifying SMR modulations linked to different mental states starts with the computation of the CSP filters. To do this, the frequency band and time intervals in which the CSP filter should maximize, respectively minimize the variance for each class are selected beforehand (see 2.1). Then, CSP analysis is applied and two to three filters are selected for each class. Further, the log-variance of the CSP projections on the data corresponding to the selected filters are calculated and used as features to classify with a (regularized) linear discriminant analysis *[(R)LDA]* classifier. Note that CSP analysis uses label information, which means that CSP filters can only be calculated from calibration data, but can then be used for real-time feedback application.

The classification of SMR modulations induced by motor imagery based on CSP analysis comport many advantages including dimension reduction (less channels), high accuracy performance of a simple linear classifier and interpretability of the solutions.

2.4 Offline analysis of SMR based BCI Data

We took data from a large scale BCI study (Blankertz et al., 2010), selecting 23 naive participants who reached at least 70% accuracy in left vs. right hand BCI feedback (15 females; mean age 26.7±12.2 years). For each participant, data was acquired from a single BCI session consiting of a *calibration* phase (motor imagery without feedback) and a *feedback* phase (motor imagery with feedback). Figure 4 describes a typical trial from both phases.

For each trial, the *SMR Pow* value of the prestimulus interval -1000 to 0 ms was computed. Two groups of trials were created according to the 60^{th} and 40^{th} percentiles of the *SMR Pow* averaged over all trials: the *high*-group displayed an *SMR Pow* value higher than the 60^{th} percentile and the *low*-group, a value lower than the 40^{th} percentile. A subject-specific

classifier based on CSP analysis (see section 2.3 and (Blankertz et al., 2008)) was trained on the calibration data and applied to windows of 1000 ms duration sliding over the motor imagery period of the feedback trials.

2.5 Online setting incorporating user's SMR level

10 subjects (5 females) of mean age 28.5 ± 3.2 years underwent a single BCI session consisting of an *online calibration* (CB) phase, a *feedback* (FB) phase (both consisting in motor imagery with feedback) and four intermittent *Neurofeedback training* (NFT) runs where the *SMR Ratio* was monitored and fed back to the participants in both time scales. The session also included three *rest* measurements where the participant had to sit quietly with open eyes and watch an animation gradually changing color and shape. Data from this measurement was used to select the subject-specific features (frequency bands, electrodes and SMR range) in order to train the *SMR extractor* that was used to monitor the SMR during the NFT and the *feedback* runs.

The classifier was adapted after each trial using a co-adaptive learning method following (Vidaurre, Sannelli, Müller, & Blankertz, 2010). This allowed us to provide the user with feedback from the start of the session. We recorded 160 calibration trials acquired in two runs of 80 trials (15 seconds break every 20 trials) and 180 feedback trials acquired in 3 blocks with 2 runs of 30 trials (15 seconds break every 15 trials). The feedback trials differed from a the standard cued motor imagery paradigm in one point: the participant's actual *SMR Ratio* (averaged over the short time scale) controlled the timing of cue presentation by exceeding, respectively falling below, a *high*, repectively *low* threshold. This introduced a variable *waiting time* before the trial start. The thresholds were determined by the 15^{th} and 85^{th} percentiles of the extracted *SMR Ratio* during the NFT period precending the *feedback* block, yielding the *high* and *low* conditions and were updated three times through the session. To avoid too long waiting times, thresholds were decreased/increased after 20 seconds reaching zero or one after 30 seconds. In total, we recorded 120 trials (4 runs) for the *high* condition and 60 trials (2 runs) for the *low* condition. Figure 5 describes the different steps and phases of the online BCI setting.

3 Results

3.1 Offline study

Figure 6 displays the grand average classification error computed in each 1000 ms window for both trial groups. A Wilcoxon signed rank test is performed to assess the differences in classification rates for both groups at each point in time and the obtained p-values are gradually represented with a pink scale. We found that the classification error was lower for the *high*- compared to the *low*-group over the whole trial length. This decrease was significant in an interval ranging from approximately 500 to 3200 ms ($p < 0.05$) after the apparition of the cue. However, the main effect was observed in a smaller interval (approximately 500 to 2500 ms).

In order to quantify the effect of the trial-separation using the *SMR Pow* methods on the classification performance, figure 7 shows the correlation between the *classification gain* and a

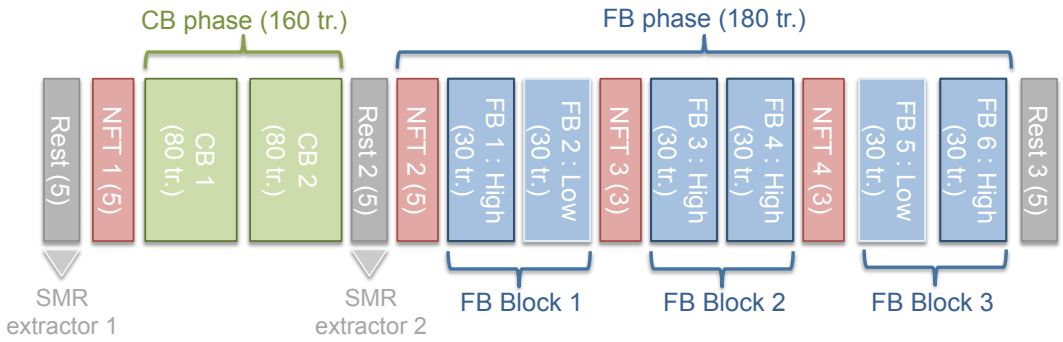

Figure 5: Schematic description of our online BCI experiment incorporating the user's current SMR level. The whole session consisted of 3 Rest measurement runs of 5 minutes each (gray), 4 NFT runs of 3-5 minutes (red), 2 calibration (CB) runs of 80 trials each (green) and 3 feedback (FB) blocks (blue) each consisting of 2 feedback runs of 30 trials each. The timing (in minutes) and the number of trials (tr.) is indicated in brackets.

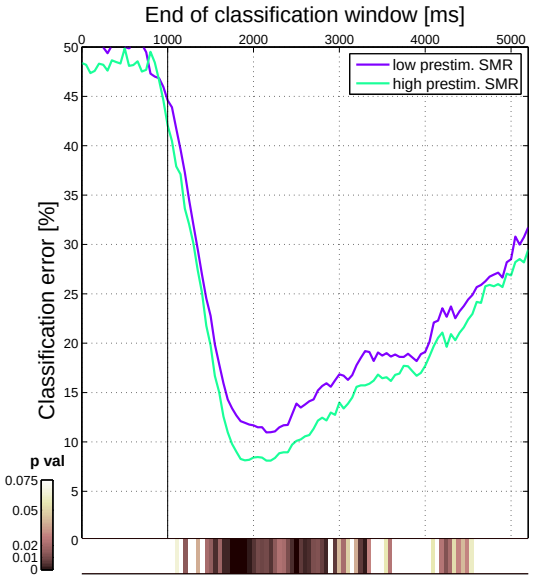

Figure 6: Monitoring of grand average classification error over the whole trial in 1000 ms windows (50 ms overlap) for both trial groups (*high*: green, *low*: purple). The pink scale represents the p-values obtained from a Wilcoxon signed-ranked test for difference in classification error.

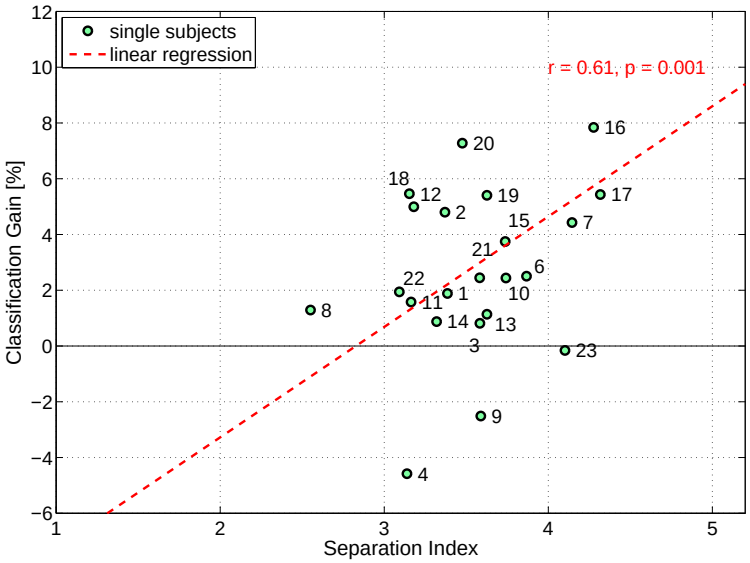

Figure 7: Correlation between the average *classification gain* in the post-stimulus window (500-2500 ms) and *separation index* according to pre-stimulus log band power value. The green dots represent the values for the single participants and the red dotted line shows the result of a linear regeression. The correlation value (r) and the corresponding p-value (p) are displayed in red.

separation index. The *classification gain* is calculated by subtracting the average classification error for the *low* trial group in the post-stimulus interval (500-2500 ms) from the one for the *high* trial group and is quantified in %. The *separation index* represents the distance between both trial group means compared to their standard deviation using the *SMR Pow* method and is calculated in the following way:

$$\frac{\mu_{high} - \mu_{low}}{\frac{1}{2}(std_{high} + std_{low})} \tag{1}$$

μ being the mean of the specific trial group and *std* its standard deviation.
We report a significant correlation between the *separation index* and the *classification gain* ($r = 0.61$, $p = 0.001$). The corresponding linear regression is shown as a red dotted line. This means that a strong difference in pre-stimulus SMR level is linked to a higher gain in classification accuracy.

The right panel of figure 8 shows the temporal evolution of the SMR amplitude modulations following motor imagery in the best CSP-channels for each class. These curves were computed by calculating the envelope of the band-passed signal using a Hilbert Transform, which was then smoothened with a moving average (200 ms window). The four trial groups (two per class) are represented in both channels: left-low (light blue), left-high (dark blue), right-low (light red) and right high (dark red). We report that the main different between the *high* and the *low* trial groups can be seen in the channel-non-specific class (shaded in yellow).

The left panel of figure 8 represents scalp topographies of the p-values for the null hypothesis of zero biserial correlation between SMR band amplitude and trial group membership in

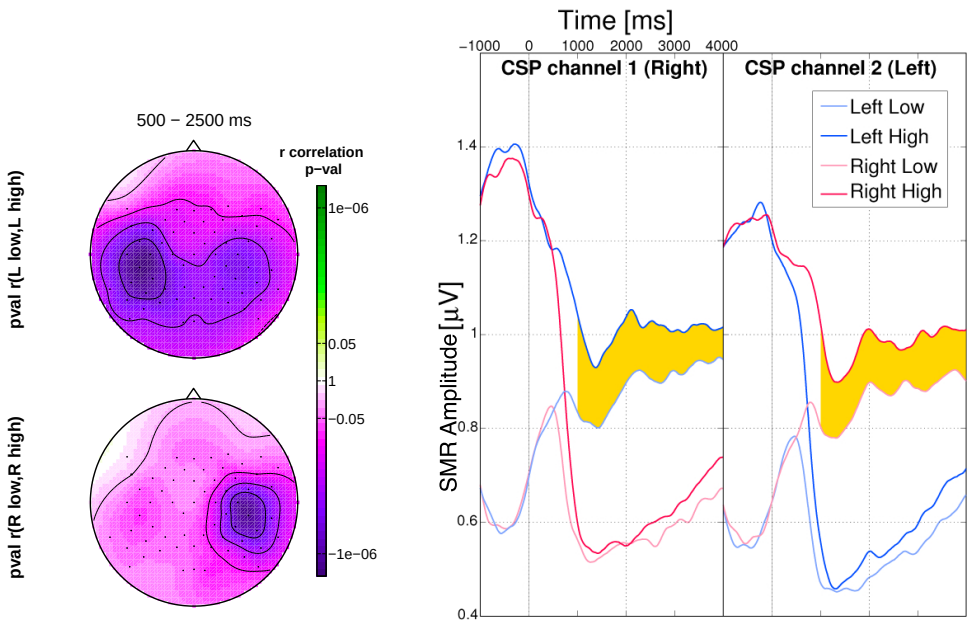

Figure 8: *Left panel*: p-values for the hypothesis of no correlation between SMR band amplitude and trial group membership in the grand average for each class: Left low vs. Left high and Right low vs. Right high. Scalp topographies are shown for the signed correlation p-values averaged over the post-stimulus (500-2500 ms) interval. Note the SMR amplitude is higher over the ipsilateral hemisphere for the *high* trial group. *Right panel:* Grand average SMR amplitude evolution over the whole trial in the two best CSP channels (one for each class). These curves are displayed for the four trial groups: left-low (light blue), left-high (dark blue), right-low (light red) and right high (dark red). Note that the highest difference occurs in the channel-non-specific class (colored in yellow).

the grand average. The correlations are computed on the envelope (see above) of the band-passed and spatially filtered (with local average reference) signals. These scalp topogrpahies are shown for the post-stimulus interval (500-2500 ms) and the *high* and *low* trial groups within each class: Left low vs Left high and Right low vs Right high.

We observe a highly significant correlation between SMR amplitude in the post stimulus interval and group membership in the ipsilateral hemisphere ($p < 10^{-6}$).

Altogether, figure 8 demonstrates that the main effect of the two different background states *high* and *low* on the motor imagery period refers to the ipsilateral motor area: the SMR level remains higher in the *high* prestimulus state, while the difference on the contralateral side only persists weakly.

3.2 Online setting incorporating user's SMR level

From our ten participants, six performed very well ($> 85\%$). But the other four either did not achieve BCI control or did not display neurophysiological patterns. Therefore, these four participants had to be removed from the analysis, which left us only with six participants with very good BCI feedback performance.

Figure 9 shows the correlation between *classification gain* in the post-stimulus window

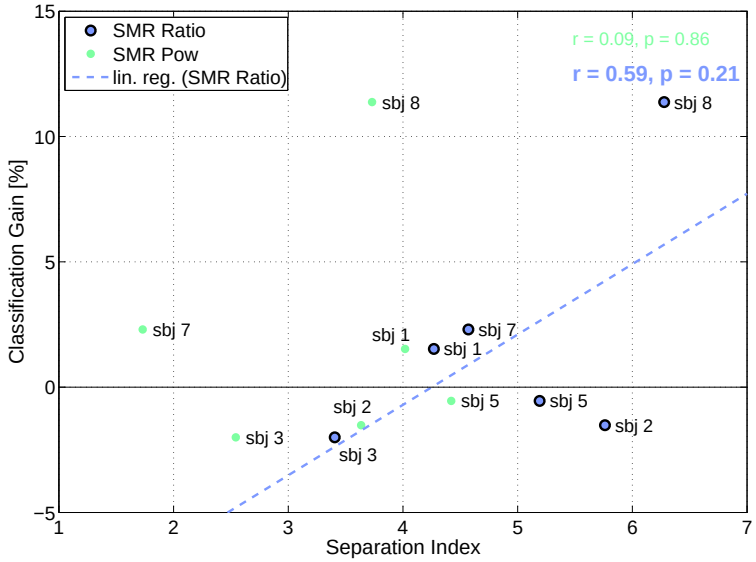

Figure 9: Correlation between the *classification gain* in the post-stimulus window ([500 3000] ms) and *separation index* based on the *SMR Ratio* (in blue). The dots represent the values for the single participants and the dotted line shows the result of a linear regression. For comparison, the corresponding points for the *SMR Pow* are shown in green. The correlation values (r) and the corresponding p-value (p) for both methods are displayed in the appropriate group color.

([500 3000] ms) and *separation index* based on the *SMR Ratio* (in blue). For comparison, the corresponding *SMR Pow* values are shown in green. We report a correlation between *classification gain* and *separation index* computed with the *SMR Ratio* (r=0.59). Furthermore, we observe that this correlation is much weaker using the standard *SMR Pow* measurment (r= 0.09).

In order to compare the two SMR quantification measures further, figure 10 shows the mean and standard deviation *SMR Ratio* (top) and *SMR Pow* (bottom) for the trial groups corresponding to each condition. We observe that the *SMR Ratio* methods yields a stable and high separation between the trial groups for each participants and that updating the thresholds account for the small jitter in SMR level over the experiment, allowing to adapt to the participants' rest SMR level. However, when applying the *SMR Pow* measure to both trial groups, we observe discrepancies between users and a very low separation distance.

Furthermore, similar effects as shown in Figure 8 for the offline study were replicated in the online study (not shown here).

4 Discussion

4.1 Ipsilateral hemisphere idling boosts classification

We demonstrated that trials with *higher* SMR amplitude preceding motor imagery can be better classified than trials with *lower* SMR amplitude during this period. This effect was

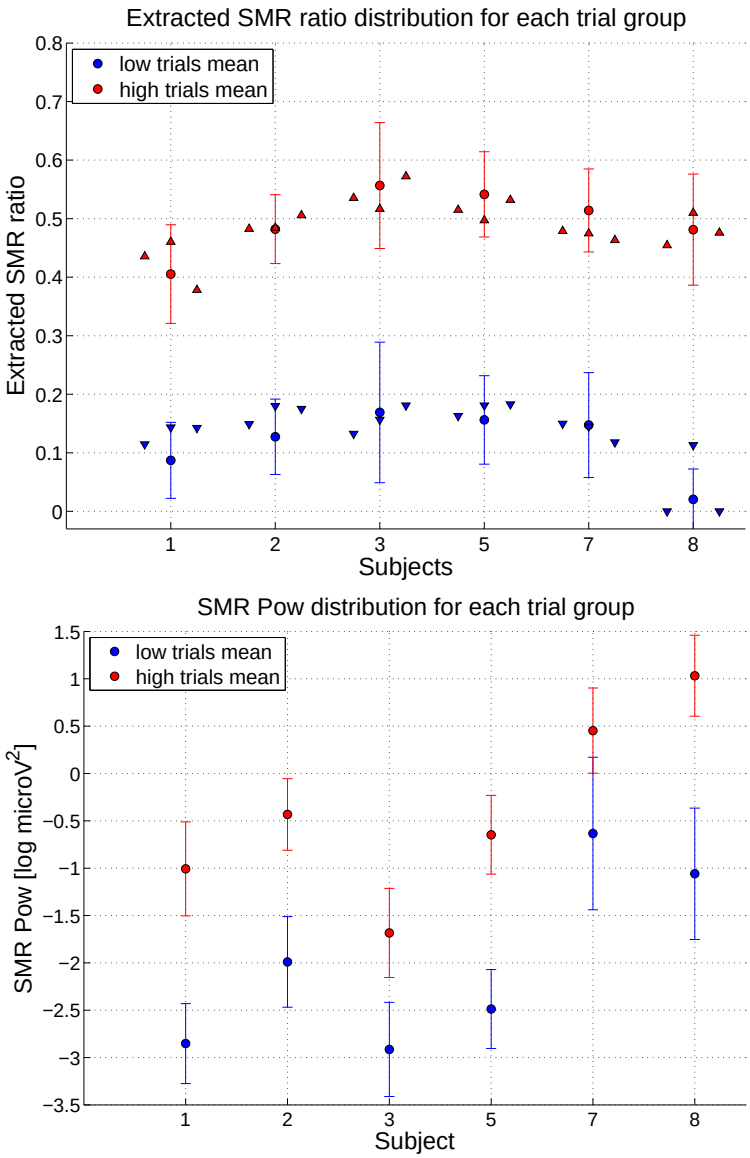

Figure 10: Average Pre-stimulus ([−750 0] ms) extracted *SMR ratio* and *SMR Pow* for the *high*(red) and *low*(blue) conditions. The mean for each trial group is represented as a dot filled with the color specific to each trial group, and the error bars show the standard deviation. For the *SMR Ratio*, the red triangles depict the threshold each subject's SMR had to reach to start the trial in the *high* condition for each block of two runs, and the same goes for the blue triangles in the *low* condition. Note that the *SMR Pow* measure includes a logarithmic scaling, which is not the case of the *SMR Ratio*.

significant in the time interval corresponding to the ERD and suggests that the ongoing SMR amplitude has an effect on the ERD/ERS patterns induced by motor imagery.

Further investigation provided more insights into the spatiotemporal evolution of the SMR fluctuations. Surprinsingly, they did not attribute the increase in classification for trials with *higher* pre-stimulus SMR level to a stronger attenuation of the SMR (ERD) in the contralateral hemisphere, but to the persistance of a higher SMR level over the ipsilateral hemisphere. Based on evidence that an increase in SMR amplitude is preceded by muscle tone reduction (Chase & Harper, 1971), we expect this effect to be due to a better relaxation state of the sensorimotor system. In addition, (Mazaheri et al., 2009) showed that high power in the α frequency band over the motor cortex makes it immune to external inputs by increasing its excitation threshold. Hence, we hypothetize that a better state of relaxation in the motor cortices leading to higher SMR amplitude, will result in an ERD focalized to the task relevant (contralalteral) cortical area accompagnied by an ERS (idling) over the other areas. This hypothesis is in line with (Neuper, Schlögl, & Pfurtscheller, 1999), who observed that the ipsilateral localized ERS often develops as the number of BCI training sessions with feedback increase and is further associated with and increase in the classification accuracy. This could be an effect of the subject getting used to the task and/or developing a skill and hence could be linked to both motor cortex and cognitive relaxation. Further supporting our findings, (Neuper et al., 1999) also observed that the development of this contralateral ERD / ipsilateral ERS pattern is associated with an increase in classification accuracy.

Due to the well documented attenuation of rhythmic activity in contralateral motor areas following unilateral upper-limb motor intentions (Pfurtscheller & Aranibar, 1979; Pfurtscheller & Neuper, 1997), research on SMR based BCIs has mainly focused on the contralateral hemisphere. However, here, we provide evidence that the ipsilateral hemisphere also contains valuable information for decoding mental states. In line with our results, an Electrocorticography (ECoG) study by Gangly et al. (Ganguly et al., 2009) reported cortical field potentials that correlated with ipsilateral kinematics. Recent studies have also demonstrated that chronic stroke patients with limb paralysis can use nonivasively recorded ipsilateral SMR modulations to achieve BCI control (Buch et al., 2008) and that the ones who achieve a high level of recovery often display increased ipsilateral activation during movement (Riecker et al., 2010). Alltogether, this supports the idea that alternative signals can be used for BCI control, when the regular signals cannot be recorded.

4.2 Including SMR monitoring in a SMR-based BCI setting

The main idea behind manipulating the cue presentation was to restrict participants' motor imagery performance to the opportunity window where their motor cortex is relaxed enough and thus in the best state to yield good classifiable ERD/ERS patterns. The goal of this manipulation was to avoid users to produce unappropriate activation patterns due to muscular tension (leading to desychronization of task unrelated motor areas) or difficulties when switching between tasks as was reported by (Sannelli, Braun, & Müller, 2009). However, this would only be useful for medium BCI performers users who do not already have high control on the timing and localization of their (de)synchronization. As none of the ten participants belonged to the target group of users, it was difficult to assess the effect of our manipulation on classification performance. Nevertheless, we still identified the same increase in ipsilateral hemisphere SMR activity between the *high* and *low* pre-stimulus SMR conditions. The aver-

age effect over the six selected participants is of course smaller than in the offline analysis, but when looking more in detail, we report that the participants exhibiting the highest increase in classification accuracy are also the ones displaying the highest difference in ipsilateral hemisphere activity in the post-stimulus interval. This makes sense, as the users with very good control over their ERD/ERS might not display this asymmetry in ipsilateral activity between the two conditions, because they are able to induce balanced ERD/ERS patterns even when their motor cortex is not in the most adequate state.

Online quantification of the SMR level can suffer extensively from the non-stationarities of the EEG signal. These include inter-subject variability and artifact sensitivity of the EEG spectrum (Barlow, 1986; Berkhout & Walter, 1968; Oken & Chiappa, 1988), which results in single participant's spectra having both different baseline activity levels and shapes.

For example, if one individual's spectrum has a generally high overall power, even a big SMR peak will not contribute much to the SMR amplitude compared to the overall activity. When we then compare the amplitude in the SMR band, the difference between the trials can be very small although an important peak to peak difference is observed. Consecutively, it is difficult to attribute an observed difference to a real variation in peak amplitude, as it could as well be attributed to a variation in overall activity.

By developing an algorithm to extract the *SMR Ratio*, we hoped to prevent the non-stationarities of the EEG signal to affect our quantification of the SMR level by extracting only the SMR peak amplitude. This was successful, as we achieved the same high separation distance between trial groups for all participants, compared to the *SMR Pow* method which yielded inhomogeneous results. Furthermore, the classification gain between the two conditions in the online experiment correlated better with the *SMR Ratio*, than the *SMR Pow* for these trials groups, which means that our new SMR quantification measure is more stable and reflects neurophysiological mechanisms.

5 Conclusion

In this study, we showed that the mental state of a BCI user can influence performance in an SMR-BCI setting. More precisely, higher SMR amplitudes over the motor areas linked to motor relaxation induce better classifiable brain patterns. Interestingly, this increase in performance can be attributed to the ipsilateral, rather than the contralateral hemisphere. Here we present an approach to use this information in an online setting, in order to boost classification. However, as none of the ten participants belonged to the target group of medium BCI performers, a large scale study is required for evaluation.

6 Acknowledgements

I would like to address special thanks to my supervisor Dr. Benjamin Blankertz for his support and motivation for my study. Many thanks also to Claudia Sannelli and Stefan Haufe for the time they invested in helping me out with theoretical, as well as practical issues. Finally, I would also like to thank the whole BBCI group for such a nice working atmosphere and great discussions in the *Panorama Büro*.

References

Barlow, J. (1986). Artifact processing (rejection and minimization) in EEG data processing. In *Lopes da silva f.h., storm van leeuwen w., remond a., editors. handbook of electroencephalography and clinical neurophysiology* (Vol. 2, pp. 15–62). Amsterdam: Elsevier.

Berkhout, J., & Walter, D. (1968). Temporal stability and individual differences in the human EEG- An analysis of variance of spectral values(Temporal stability and individual differences in human EEG from variance analysis of normalized power spectra data under rest and perceptual stress conditions). *IEEE Transactions on Bio-Medical Engineering*, *15*, 165–168.

Blankertz, B., Dornhege, G., Krauledat, M., Schröder, M., Williamson, J., Murray-Smith, R., et al. (2006). The Berlin brain-computer interface presents the novel mental typewriter hex-o-spell. In *Proceedings of the 3rd international brain-computer interface workshop and training course* (pp. 108–109).

Blankertz, B., Krauledat, M., Dornhege, G., Williamson, J., Murray-Smith, R., & Müller, K. (2007). A note on brain actuated spelling with the Berlin Brain-Computer Interface. *Universal Access in Human-Computer Interaction. Ambient Interaction*, 759–768.

Blankertz, B., Sannelli, C., Halder, S., Hammer, E., Kübler, A., Müller, K., et al. (2010). Neurophysiological predictor of SMR-based BCI performance. *NeuroImage*, *51*(4), 1303–1309.

Blankertz, B., Tangermann, M., Vidaurre, C., Dickhaus, T., Sanelli, C., Popescu, F., et al. (2009). Detecting Mental States by Machine Learning Techniques: The Berlin Brain-Computer Interface. In *Non-invasive and invasive brain-computer interfaces.* Springer, The Frontiers Collection.

Blankertz, B., Tomioka, R., Lemm, S., Kawanabe, M., & Müller, K. (2008). Optimizing spatial filters for robust EEG single-trial analysis. *IEEE Signal Processing Magazine*, *25*(1), 41–56.

Buch, E., Weber, C., Cohen, L., Braun, C., Dimyan, M., Ard, T., et al. (2008). Think to move: a neuromagnetic brain-computer interface (BCI) system for chronic stroke. *Stroke*, *39*(3), 910–917.

Chase, M., & Harper, R. (1971). Somatomotor and visceromotor correlates of operantly conditioned 12-14 c/sec sensorimotor cortical activity. *Electroencephalography and clinical neurophysiology*, *31*(1), 85–92.

Del Percio, C., Marzano, N., Tilgher, S., Fiore, A., Di Ciolo, E., Aschieri, P., et al. (2007). Pre-stimulus alpha rhythms are correlated with post-stimulus sensorimotor performance in athletes and non-athletes: a high-resolution EEG study. *Clinical Neurophysiology*, *118*(8), 1711–1720.

Dijk, H. van, Schoffelen, J., Oostenveld, R., & Jensen, O. (2008). Prestimulus oscillatory activity in the alpha band predicts visual discrimination ability. *Journal of Neuroscience*, *28*(8), 1816–1823.

Enzinger, C., Ropele, S., Fazekas, F., Loitfelder, M., Gorani, F., Seifert, T., et al. (2008). Brain motor system function in a patient with complete spinal cord injury following extensive brain–computer interface training. *Experimental Brain Research*, *190*(2), 215–223.

Ergenoglu, T., Demiralp, T., Bayraktaroglu, Z., Ergen, M., Beydagi, H., & Uresin, Y. (2004). Alpha rhythm of the EEG modulates visual detection performance in humans. *Cognitive Brain Research*, *20*(3), 376–383.

Fukunaga, K. (1990). *Introduction to statistical pattern recognition.* Academic Pr.

Ganguly, K., Secundo, L., Ranade, G., Orsborn, A., Chang, E., Dimitrov, D., et al. (2009). Cortical representation of ipsilateral arm movements in monkey and man. *Journal of Neuroscience*, *29*(41), 12948–12956.

Hanslmayr, S., Klimesch, W., Sauseng, P., Gruber, W., Doppelmayr, M., Freunberger, R., et al. (2005). Visual discrimination performance is related to decreased alpha amplitude but increased phase locking. *Neuroscience letters*, *375*(1), 64–68.

Hanslmayr, S., Sauseng, P., Doppelmayr, M., Schabus, M., & Klimesch, W. (2005). Increasing individual upper alpha power by neurofeedback improves cognitive performance in human subjects. *Applied psychophysiology and biofeedback*, *30*(1), 1–10.

Hummel, F., Andres, F., Altenmuller, E., Dichgans, J., & Gerloff, C. (2002). Inhibitory control of acquired motor programmes in the human brain. *Brain*, *125*(2), 404.

Klimesch, W. (1999). EEG alpha and theta oscillations reflect cognitive and memory performance: a review and analysis. *Brain Research Reviews*, *29*(2-3), 169–195.

Klimesch, W., Sauseng, P., & Gerloff, C. (2003). Enhancing cognitive performance with repetitive transcranial magnetic stimulation at human individual alpha frequency. *European Journal of Neuroscience*, *17*(5), 1129–1133.

Klimesch, W., Vogt, F., & Doppelmayr, M. (1999). Interindividual Differences in Alpha and Theta Power Reflect Memory Performance. *Intelligence*, *27*(4), 347–62.

Koles, Z. (1991). The quantitative extraction and topographic mapping of the abnormal components in the clinical EEG. *Electroencephalography and Clinical Neurophysiology*, *79*(6), 440–447.

Mazaheri, A., Nieuwenhuis, I., Dijk, H. van, & Jensen, O. (2009). Prestimulus alpha and mu activity predicts failure to inhibit motor responses. *Human brain mapping*, *30*(6), 1791–1800.

Millàn, J. d. R., Renkens, F., Mouriño, J., & Gerstner, W. (2004). Non-Invasive Brain-Actuated Control of a Mobile Robot by Human EEG. *IEEE Trans. on Biomedical Engineering Volume*, *51*(6), 1026–1033.

Neuper, C., & Pfurtscheller, G. (2001). Event-related dynamics of cortical rhythms: frequency-specific features and functional correlates. *International Journal of Psychophysiology*, *43*(1), 41–58.

Neuper, C., Schlögl, A., & Pfurtscheller, G. (1999). Enhancement of left-right sensorimotor EEG differences during feedback-regulated motor imagery. *Journal of Clinical Neurophysiology*, *16*(4), 373–382.

Oken, B., & Chiappa, K. (1988). Short-term variability in EEG frequency analysis. *Electroencephalography and clinical Neurophysiology*, *69*(3), 191–198.

Palva, S., & Palva, J. (2007). New vistas for [alpha]-frequency band oscillations. *Trends in neurosciences*, *30*(4), 150–158.

Pfurtscheller, G., & Aranibar, A. (1979). Evaluation of event-related desynchronization (ERD) preceding and following voluntary self-paced movement. *Electroencephalography and clinical neurophysiology*, *46*(2), 138–146.

Pfurtscheller, G., Guger, C., Müller, G., Krausz, G., & Neuper, C. (2000). Brain oscillations control hand orthosis in a tetraplegic. *Neuroscience letters*, *292*(3), 211–214.

Pfurtscheller, G., Leeb, R., Keinrath, C., Friedman, D., Neuper, C., Guger, C., et al. (2006). Walking from thought. *Brain Research*, *1071*(1), 145–152.

Pfurtscheller, G., & Neuper, C. (1997). Motor imagery activates primary sensorimotor area in humans. *Neuroscience letters*, *239*(2-3), 65–68.

Pfurtscheller, G., Neuper, C., Flotzinger, D., & Pregenzer, M. (1997). EEG-based discrimination between imagination of right and left hand movement. *Electroencephalography and clinical Neurophysiology*, *103*(6), 642–651.

Pfurtscheller, G., & Silva, F. Lopes da. (1999). Event-related EEG/MEG synchronization and desynchronization: basic principles. *Clinical Neurophysiology*, *110*(11), 1842–1857.

Riecker, A., Gröschel, K., Ackermann, H., Schnaudigel, S., Kassubek, J., & Kastrup, A. (2010). The role of the unaffected hemisphere in motor recovery after stroke. *Human brain mapping*, 1017–1029.

Sannelli, C., Braun, M., & Müller, K. (2009). Improving BCI performance by task-related trial pruning. *Neural Networks*, *22*(9), 1295–1304.

Suffczynski, P., Kalitzin, S., Pfurtscheller, G., & Silva, F. Lopes da. (2001). Computational model of thalamo-cortical networks: dynamical control of alpha rhythms in relation to focal attention. *International Journal of Psychophysiology*, *43*(1), 25–40.

Vidaurre, C., Sannelli, C., Müller, K., & Blankertz, B. (2010). Machine learning based co-adaptive learning: Towards a cure for BCI illiteracy. *submitted*.

Zhang, Y., & Ding, M. (2010). Detection of a weak somatosensory stimulus: Role of the prestimulus mu rhythm and its top–down modulation. *Journal of Cognitive Neuroscience*, *22*(2), 307–322.